Smart Structures and Systems, *Vol. 15, No. 4 (2015) 963-995*
DOI: http://dx.doi.org/10.12989/sss.2015.15.4.963

Shaking table testing of a steel frame structure equipped with semi-active MR dampers: comparison of control algorithms

N. Caterino[*1], M. Spizzuoco[2a] and A. Occhiuzzi[1,3b]

[1]*Department of Engineering, Università degli Studi di Napoli Parthenope, Naples, Italy*
[2]*Department of Structures for Engineering and Architecture, Università degli Studi di Napoli Federico II, Naples, Italy*
[3]*Construction Technologies Institute ITC-CNR, San Giuliano Milanese, Milan, Italy*

(Received June 27, 2013, Revised February 10, 2014, Accepted February 16, 2014)

Abstract. The effectiveness of the various control algorithms for semi-active structural control systems proposed in the literature is highly questionable when dealing with earthquake actions, which never reach a steady state. From this perspective, the paper summarizes the results of an experimental activity aimed to compare the effectiveness of four different semi-active control algorithms on a structural mock up representative of a class of structural systems particularly prone to seismic actions. The controlled structure is a near full scale 2-story steel frame, equipped with two semi-active bracing systems including two magnetorheological dampers designed and manufactured in Europe. A set of earthquake records has been applied at the base of the structure, by utilizing a shaking table facility. Experimental results are compared in terms of displacements, absolute accelerations and energy dissipation capability. A further analysis on the percentage incidence of undesired and/or unpredictable operations corresponding to each algorithm gives an insight on some factors affecting the reliability and, in turn, the real effectiveness of semi-active structural control systems.

Keywords: semi-active control; shaking table test; magnetorheological damper; control algorithms; smart device

1. Introduction

Generally speaking, structural control is aimed to bound the structural response to a pre-assigned level. According to the specific structural problem, various techniques and technologies have been proposed in the last decades. Among them, structural control of seismic response through the adoption of semi-active (SA) systems based on magnetorheological (MR) dampers is the specific subject of this paper. The specialty of this class of problems is related both to the external excitation, which is typically significant for short to medium height buildings and highway viaducts, and to the SA devices considered. Obviously, tall structures, whose dynamics fall outside the range of the significant part of earthquake bandwidth, are beyond the scope of this

∗Corresponding author, Assistant professor, E-mail: nicola.caterino@uniparthenope.it
[a] Assistant professor
[b] Professor

http://www.techno-press.org/?journal=sss&subpage=8 ISSN: 1738-1584 (Print), 1738-1991 (Online)

paper.

Typically, SA structural control systems rely on smart devices able to provide a rapid variation of their stiffness and/or damping properties. Although the probably first implementation of a SA structural control system is based on variable stiffness devices (Kobori *et al.* 1993), today most of the research efforts are aimed to the adoption of variable damping schemes. The latter idea was first introduced in the early 1970s by Crosby and Karnopp (1973), who showed the possibility of exploiting a variable-constant viscous damper in the context of automotive industry. The original work of Crosby and Karnopp envisioned a SA suspension driven by a two-state switching policy that makes the viscous damper behave pretty much like a sky-hook device. One of the advantages of such idea is the corresponding model-free control algorithm, whose implementation does not require a previous knowledge of the system parameters and/or of the external excitation (Cao *et al.* 2011). A number of scientific papers have subsequently proposed many different ideas to define control algorithms for SA control systems. However, all the proposals can be considered belonging to one of the following families:

- Control algorithms derived from a known control theory applied to provide a full control authority. In this case, SA devices are looked at as - purely reactive - force actuators and the full control authority has to be clipped in order to match the effective capabilities of the dampers;
- Control algorithms based on a sound physical sense, where SA devices are typically seen as smart damping devices for which the amount of dissipation can be quickly regulated.

Control algorithms belonging to the 1st family (known control theory) usually requires real time estimates of the full system state. These estimates can come from a full state measurement or from state observers, i.e. numerical models of the real structure running in parallel to it and able to estimate the full system state based on measurements of a limited set of state variables, provided that a good model of the structure to protect be available. In the case of civil structures, this corresponds to real time evaluation of displacements and velocities at every degree of freedom (DOF). However, direct measurement of displacement and velocity is seldom a viable opportunity: typical dynamic acquisitions on civil structures rely on accelerometric recording. The calculation of displacements and velocities from accelerations can be done either by on line double integration or, again, through the adoption of state observers.

Control algorithms belonging to the 2nd family (sound physical sense) are typically simpler than their counterparts of the 1st family and usually require less measurements, which are often made in the close surroundings of the devices. The corresponding computational effort is fairly moderate. Apart from the initial, bi-state and coefficientless control algorithm suggested by Crosby and Karnopp, some other different proposal, based on a clear physical sense, can be found in the scientific literature. Inaudi (1997) proposed a control strategy for SA friction dampers, based on the concept that a variable friction coefficient has to be adjusted so as to be proportional to the deformation of the device itself. A modified version of this controller for variable-damping device is shown in (Inaudi 2000). The original idea of Inaudi was subsequently developed in a more complex control algorithm taking into account both relative displacement and velocity of the damper (Xu and Chen 2008). Stammers and Sireteanu (1998), in the context of vehicle suspension design, introduced a control algorithm for SA friction dampers aimed to reduce the accelerations of the main body of a car. They extended their idea to the case of seismic structures in Stammers and Sireteanu (2000). Many authors (Yang *et al.* 2000, Yang and Agrawal 2002, Barroso *et al.* 2003, Erramouspe *et al.* 2007) have proposed a resetting control scheme to drive SA dampers. The resetting principle is based on the introduction of a SA bracing system, to be considered as an

energy extractor, composed by an elastic element and a damping device. The elastic element is adopted to temporarily store strain energy to be quickly damped out during short dissipation cycles. Resetting systems can be analyzed in the framework of control theory, as shown by Occhiuzzi and Spizzuoco (2005). Other control logics based on physical concepts are shown in (Sodeyama *et al.* 2004, Jung *et al.* 2004, 2008, Weber *et al.* 2009, Laflamme *et al.* 2011).

Although these control algorithms are widely described in the scientific literature, their effectiveness is almost always shown by numerical applications. Notable exceptions are cited in the following. Li and Xu (2004) performed shaking table tests on a three-story one-bay frame model, controlled by a double-ended shear mode combined with valve mode MR fluid device placed between the ground and the first floor. The validity of the SA control system was verified by implementing three different control algorithms: the instantaneous optimal control algorithm, the classical linear optimal control algorithm, and the linear-quadratic Gaussian control algorithm. Lee *et al.* (2010) adopted a full-scale five-story testing structure to make an experimental comparison of different SA algorithms (Lyapunov algorithm, neuro-control logic, maximum energy dissipation algorithm) to control the behavior of the MR damper-based system, under the effect of four historical earthquakes and one artificial seismic input. Basili *et al.* (2013) carried out shaking table tests to verify the effectiveness of a SA MR damper system in reducing seismic vibrations of adjacent structures. The physical model is represented by two 1:5 scaled steel structures connected at the second level by a commercial MR damper driven by an on-off control algorithm derived from the Lyapunov stability theory. Cha *et al*. (2013) presented a comparison among response reduction performances of three SA control algorithms for use with MR dampers: the clipped-optimal controller, the decentralized output feedback polynomial controller, and the simple passive controller. Real-time hybrid tests under four different earthquakes were carried out by considering an analytical building model and two physical models of large-scale MR dampers stroked by hydraulic actuators.

The present paper describes the main results of a series of tests done on a nearly-full scale steel structure equipped with 2 SA MR dampers driven by 4 different control algorithms belonging to the 2nd family introduced above. All of them require only few and local measurements of the system instantaneous response to seismic actions. Furthermore, all the algorithms do not require a previous knowledge of the dynamic characteristics of the hosting structure. The scope of the paper is:

- To highlight the different effectiveness of such algorithms, as well as the way they actually operate in driving the MR dampers;
- To point out the operating difficulties of each algorithm and the corresponding malfunctioning during the short time intervals when they are most needed, i.e., during the strong phase of an earthquake event.

2. Experimental setup

A wide experimental campaign has been conducted in the framework of the JETPACS (Joint Experimental Testing on Passive and semi-Active Control Systems (Dolce *et al*. 2008)) Program financed by the 2005-2008 ReLUIS Executive Project sponsored by the Italian Department of Civil Protection. In the following, the main features of the JETPACS structural mock up are introduced as well as its dynamic identification. Then the MR dampers adopted in the tests are briefly described, with references to papers devoted to their characterization. Finally the electronic

equipment needed to make the SA control system work is introduced, also allowing to highlight specific aspects of such kind of experimentation unusual for any other type of structural testing.

2.1 The JETPACS steel structure

The steel frame object of seismic experimental analysis is a 1:1.5 scale 2-storey one-bay steel frame with composite steel-reinforced concrete slabs (Figs. 1-3). The mock-up structure dimensions are 3 m × 4 m (plan) with a total height of about 4.5 m; four columns with HEB140 profile are placed at the corners with their flanges oriented parallel to the transverse (Y) direction. Four lateral beams (section IPE180), welded to the columns, are placed at first and second floor, whereas four lateral beams (HEB220) comprise the ground floor. Additionally, a horizontal bracing (HEA160) is provided on the horizontal plane at the ground floor. All structural elements are made of S235 steel. A concrete slab supported by coffer steel (section A55/P600) with 0.8 mm thickness is placed at the first and second floor. Additional concrete blocks (Fig. 1) raise the overall mass so as to match the design period of vibration (four blocks, 340 kg each, per floor).

The frame is supported on special sliding 1D guides positioned under the base beams, close to the column location, which allow the frame to move in the longitudinal (X) direction only.

Four chevron-type bracings (HEA100 profile) are mounted along the longitudinal direction, two for each storey. The two MR devices adopted in this research were installed at the first storey, one for each side (West and East) of the frame.

The structure adopted in the experimental campaign well represents a typical real-world situation of a short to medium height structure (the class of buildings which are more prone to suffer the effects of the earthquakes) retrofitted through a limited number of supplemental damping devices.

The dynamic characterization of the structure is described in (Antonacci *et al.* 2012, Gattulli *et al.* 2009, De Stefano *et al.* 2008) and herein only briefly summarized.

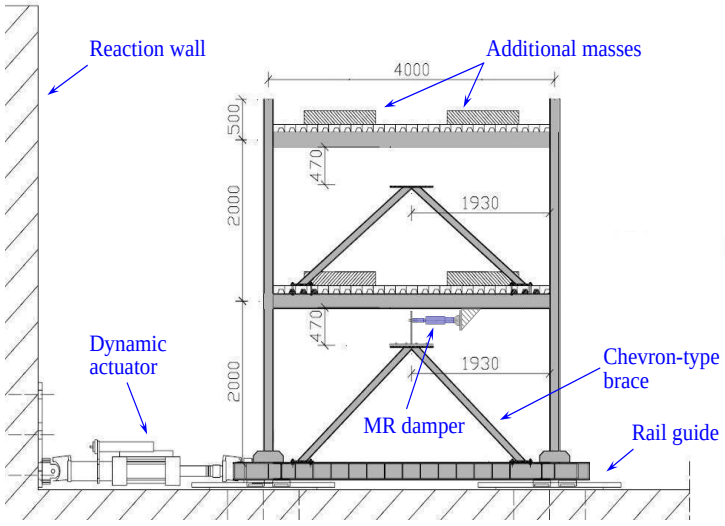

Fig. 1 Experimental setup for the JETPACS structure: lateral view (dimensions in millimetres)

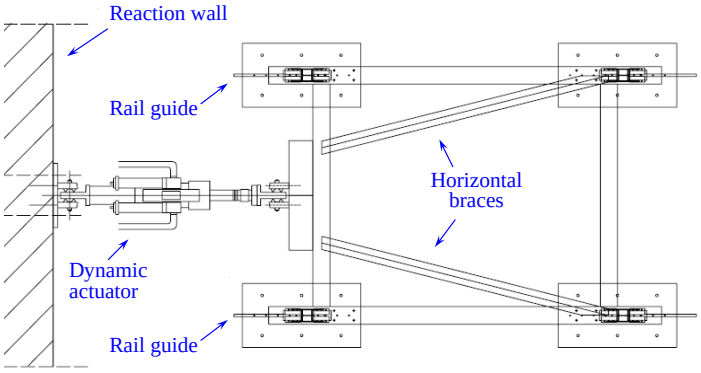

Fig. 2 Plan view of the JETPACS structure

Fig. 3 A photo of the JETPACS steel frame structure

Antonacci *et al.* (2012) presented a modal identification analysis of the JET-PACS structure conducted via four different techniques, adequately discussed and compared in term of results. Some of these techniques below to the time domain family (ERA - Eigensystem Realization Algorithm, SSI-Stochastic Subspace Identification), other to the frequency domain type (EFDD - Enhanced Frequency Domain Decomposition); the remaining (TFIE - Time Frequency Instantaneous Estimators) can be labeled as a time-frequency domain method.

Table 1 EFDD identification of the JETPACS structure

Mode	f [Hz]	T [s]	ξ [%]	Dominant component	Displacements/rotation of storeys
I	2.850	0.351	0.092	Translation Y	In-phase
II	3.577	0.280	0.153	Translation X	In-phase
III	5.107	0.196	0.073	Torsional	In-phase
IV	8.420	0.119	0.180	Translation Y	Counter-phase
V	12.380	0.081	0.130	Translation X	Counter-phase
VI	16.224	0.062	0.075	Torsional	Counter-phase

By using each of these procedures, the cited authors have obtained similar results about natural frequencies, modal damping ratios, and modal shapes of the reference structure.

Herein only the results by EFDD (having a very long tradition in the structural engineering field) are reported, for sake of brevity (Table 1). Modal shapes are uncoupled and aligned with the principal directions of the frame. In particular, the six modes correspond to a couple of translational modes and a torsional mode with in-phase (lower modes) or counter-phase (higher modes) displacement of the stories.

2.2 Magnetorheological dampers: description and identification

The devices adopted for the tests were two full-scale prototype SA MR dampers (Fig. 4) designed and manufactured by the German company Maurer Söhne. The overall dimensions of each device are 675 mm (length) ×100 mm (external diameter), with a mass of about 16 kg. A maximum force of about 30 kN can be developed along the longitudinal axis, whereas the presence of special spherical pin joints at both ends prevents the rise of bending, shear and torsional moment in the piston rod. The dampers have a stroke of ± 25 mm. The external diameters of the piston head and of the piston rod are 100 mm and 64 mm respectively. A magnetic circuit composed by coils, in series with a global resistance of 3.34 Ω, can generate the magnetic field in the device. The current in the circuit is provided in the range 0÷3 A by a specific power supply described in the following.

The devices connected the base and the first floor of the frame through the chevron type braces described above. Depending on the presence of a stiffening plate (of triangular shape; Fig. 5(a)) above each brace, behind the device, the link between each MR damper to the lower beam can be considered as (practically) rigid or flexible respectively. In the latter configuration (Fig. 5(b)), the stiffness of the link is substantially related to that of the vertical plate mounted behind the device, that behaves like a cantilever. This has been designed in order to achieve a stiffness of the same order of magnitude of the lateral stiffness of the frame. In the following it will be highlighted that some control algorithms work better if the above link is set as rigid, others if it is left flexible.

The MR dampers have been experimentally tested at the laboratory of the Department of Structural Engineering of the University of Naples Federico II (Naples, Italy) by using a specific testing apparatus. Details can be found in Caterino *et al.* (2011, 2013), including force-displacement and force-velocity loops, comparison of many different models for MR dampers, tests at different frequencies, response time of dampers (control electronics and electrical circuit) and response to step inputs.

Fig. 4 One of the two prototype MR dampers

(a) (b)

Fig. 5 Two possible configurations for the link between MR dampers and steel braces: (a) with (i.e., rigid) or (b) without (i.e., flexible) a stiffening plate behind the device

2.3 Electronic equipment

The electronic equipment adopted for the experimental activity on the JETPACS controlled by MR dampers can be distinguished in the two parts:

1. Conventional equipment for structural tests;
2. Extra-equipment for structural control.

2.3.1 Conventional equipment for structural tests

A total of 22 transducers were adopted to measure the response of the structure during the SA tests (Ponzo *et al.* 2009). The horizontal displacements of each floor were measured through four digital transducers fixed to an external steel reference frame. The floor accelerations were recorded through four X-direction horizontal, four Y-direction horizontal and one vertical accelerometers. The table-model base accelerations were recorded through two X-direction horizontal and two Y-direction accelerometers, whereas the displacement by one digital transducer, fixed to the external steel reference frame. The remaining channels were used to measure the force of the dissipating devices, by means of piezoresistive load cells mounted at the end of each device, and relative displacement, by means of four displacement transducers.

Table 2 summarizes the description of all the response parameters measured during the tests, as well as of the adopted sensors, also indicating their position in height and in plan.

2.3.2 Extra-equipment for structural control

Additional transducers have been utilized for the SA dynamic tests. Actually, this kind of experimental activity requires special attention in solving several specific aspects that characterize each of the three phases - input, processing and command - performed in each test, most of them being unusual for any other type of structural testing.

In general, during the acquisition phase, selected parameters (depending on the control algorithm adopted) of the structural response have to be continuously measured; following each measure, the processing-decision stage is performed, i.e. the measured quantities are processed by

the control algorithm in order to take the decision about the calibration of the devices; finally, the command activity has to be done, i.e., the decisions taken by the algorithm have to be transferred to the adjustable devices, by means of electrical signals and properly designed power supplies.

Table 2 Response parameters measured by University of Basilicata: description, position in height and in plan of the instruments

	Position in height (measure direction)	Position in plan	Sensor typology
Absolute horizontal displacements	Base level (X)	North side	Temposonic digit. transd., ±250mm
	1st floor (X)	East side	Temposonic digit. transd., ±250mm
	2nd floor (X)	East side	Temposonic digit. transd., ±250mm
	1st floor (X)	West side	Temposonic digit. transd., ±250mm
	2nd floor (X)	West side	Temposonic digit. transd., ±250mm
Horizontal acceleration	Base level (X)	South-East corner	Columbia servo-accelerometer, ±1 g
	Base level (Y)	South-East corner	Columbia servo-accelerometer, ±1 g
	Base level (X)	North-West corner	Columbia servo-accelerometer, ±1 g
	Base level (Y)	North-West corner	Columbia servo-accelerometer, ±1 g
	1st floor (X)	South-East corner	FGP servo-accelerometer, ±2 g
	1st floor (Y)	South-East corner	FGP servo-accelerometer, ±2 g
	1st floor (X)	North-West corner	FGP servo-accelerometer, ±2 g
	1st floor (Y)	North-West corner	FGP servo-accelerometer, ±2 g
	2nd floor (X)	South-East corner	FGP servo-accelerometer, ±2 g
	2nd floor (Y)	South-East corner	FGP servo-accelerometer, ±2 g
	2nd floor (X)	North-West corner	FGP servo-accelerometer, ±2 g
	2nd floor (Y)	North-West corner	FGP servo-accelerometer, ±2 g
Vertical acceleration	2nd floor	North side	Columbia servo-accelerometer, ±1 g
Axial displacements of devices	1st floor	East side	Penny & Giles LP displ. transd., ±50mm
	1st floor	West side	Penny & Giles LP displ. transd., ±50mm
Axial force of devices	1st floor	East side	AEP load cell, ±50 kN
	1st floor	West side	AEP load cell, ±50 kN

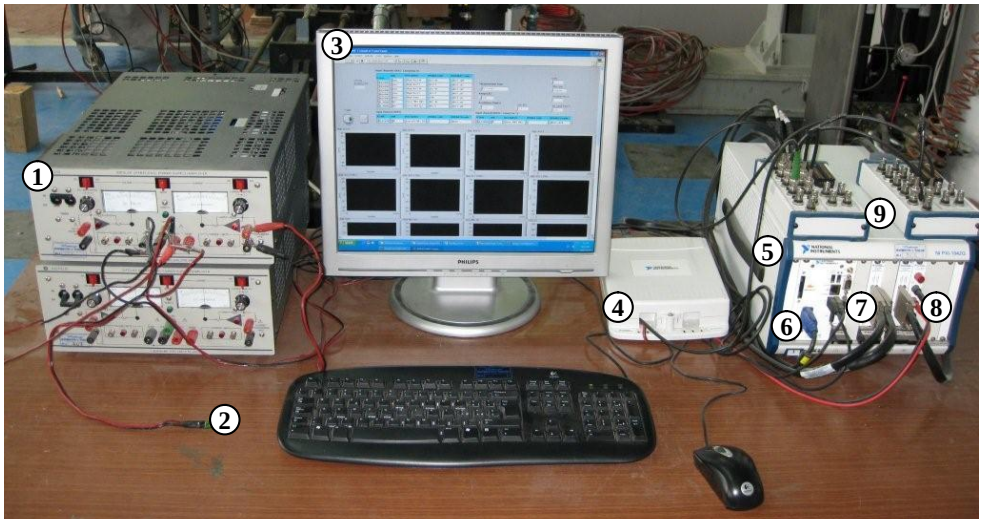

Fig. 6 Electronic equipment for acquisition and control during the JETPACS experimental tests: power suppliers (1), 1.0 μF capacitance (2), Labview software (3), voltage attenuator (4), NI chassis (5), real-time NI CPU (6), data acquisition board (7), digital multimeter (8), connectors block (9)

The special electronic equipment used to drive the SA tests is shown in Fig. 6. It includes the following components: (1) a set of two operational power supplies (model BOP 50-4 M from Kepco Inc., New York - USA), able to provide the current needed to feed the circuitry inside the MR device, featuring an output range of ±50 V, ±4 A (i.e., power source-power sink capabilities of 200 W); (2) a 1.0 μF capacitance mounted in parallel with the output (according to a specific suggestion included in the Kepco instruction manual), to the aim of stabilizing the current loop operating with inductive loads and needed to measure in real-time both the current and the voltage inside the SA MR damper; (3) the Labview Professional Development System (release 8.5), the environment in which the software needed to acquire and generate all the analog signals involved in the experimental tests was purposefully written; (4) a 10-to-1 voltage attenuator National Instruments (NI) SCC-A10 adopted to scale the ±50V output signal from the power supply to be measured by the acquisition board; (5) a chassis NI PXI 1042; (6) an embedded real-time controller NI PXI-8196 RT; (7) two NI PXI-6259 data acquisition boards each with 16 analog inputs and 4 analog outputs (±10V voltage signals, 16 bit resolution and 2800 kHz maximum sampling rate); (8) a NI PXI-4065 digital multimeter able to measure the intensity of current in the damper's circuit; (9) two connector blocks NI BNC-2110.

Each of the above-cited power sources is a fully dissipative, linear stabilizer for laboratory and systems applications: it has two bipolar control channels (voltage and current mode), selectable and individually controllable either from its front panel controls or by remote signals; each of the principal control channels is protected by bipolar limit circuits, in which the positive and negative current or voltage limit points can be manually set or remotely programmed simultaneously and individually.

Vibration periods of structures prone to earthquake effects are typically in the range 0.1~1.0 s. The bandwidth of a SA damping system must be significantly higher than the dynamics that it

intends to control. Therefore, real time modification of the damping properties of SA devices should happen in the range 1~10 ms, including both computation times and mechanical delays (Occhiuzzi *et al.* 2003, Caterino *et al.* 2011, 2013). For this reason, the sampling rate of the control system was set to 1 kHz. Furthermore, as demonstrated in Caterino *et al.* (2013), the performances of the power supply are crucial in the time response of SA MR damper. In particular, response time dramatically decreases when fluctuations of the magnetic field inside the damper are controlled by directly varying the current flowing inside the circuitry, compared to the case in which the fluctuations are controlled indirectly through imposed variations of the voltage feeding the device.

Many control algorithms proposed in literature try to include the electric dynamics of the circuitry inside MR dampers. The solution adopted for these tests is to face this dynamics by an appropriate hardware, thus reaching reaction times of the electric circuitry inside the damper well beyond 1 ms and global reaction times of the SA damper bounded to 10 ms as shown in Caterino *et al*. (2011, 2013). To achieve such objectives a current driven command scheme has been implemented, rather than a voltage driven command approach. Finally, in evaluating the different control algorithms, a negligible role to the internal dynamics of the MR dampers can be assumed.

The two MR dampers had two parallel and independent set up of sensors, cables, control algorithms and power supplies. Due to structural symmetry, data recorded for each of them were practically the same, so in the following authors will refer to any one of the two sides (West).

3. Control algorithms adopted

The SA bracing system described before has been tested while driven by 4 different control algorithms, with the aim of pointing out the different properties and effectiveness of any one of them. All of the algorithms change in real time the dynamical properties of the dampers according to the actual values of measured quantities (displacements, velocities and forces) in the close surroundings of the dampers. The original formulation of each control algorithm has been modified to be used in conjunction with SA MR dampers.

The 1st algorithm applied to the testing structure is aimed to maximize the energy extracted by the SA damper from the structure (Occhiuzzi and Spizzuoco 2005). When the force F_b acting on the SA brace and the velocity $\dot{x}_f$ of the point where the force is applied have the same sign, energy flows from the main structure into the SA damper (positive power). In these conditions, the damper should work at its maximum damping capacities, i.e., the current feeding the magnetic coils should be set to its maximum value $i_{\max}$. When the energy exchange corresponds to a negative power (energy flowing from the SA brace into the hosting structure), the damper should be set at its minimum value of the current, namely 0, so as to reduce as much as possible the power transmission to the hosting structure. This algorithm (that will be referred to as "Energy" in the following) can be described as shown below.

$$\begin{aligned} &\text{if} \quad F_b(t)\cdot \dot{x}_f(t) > 0 \quad \text{then} \quad i(t) = i_{\max} \\ &\text{if} \quad F_b(t)\cdot \dot{x}_f(t) < 0 \quad \text{then} \quad i(t) = i_{\min} = 0 \end{aligned} \tag{1}$$

For the meaning of symbols adopted here and for the following algorithms, the reader may refer to Fig. 7 that schematically represents the JETPACS structure equipped with MR dampers. at the 1st floor.

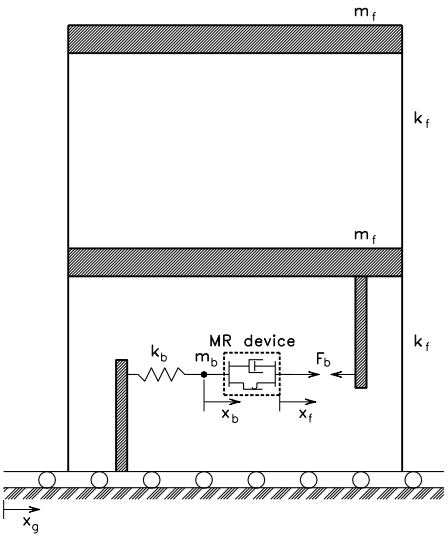

Fig. 7 Model of the tested structure

The 2nd control algorithm tested (herein referred to as "Modulated Homogeneous Friction" or simply as "MHF") tested was originally proposed by Inaudi (2000), It modulates the current into the damper according to the actual response of the structure in terms of floor displacement. It is based on the definition of the "prior-to-peak" operator "*P*" related to the interstorey drift of the first floor ($x_f - x_g$) and can be expressed as follows

$$i(t) = g \cdot |P(t)| \tag{2}$$

where g is a gain constant, whose value has been assumed for each test such that the maximum intensity of current was given when the 1st interstorey drift ratio achieved the value of 0.005 (i.e., $x_f - x_g$ = 10 mm). Therefore, in the tests the gain constant was set to $g = 0.1 i_{max}$ A/mm.

The 3rd control algorithm tested aimed to make the SA damper behave like a sky hook damper, i.e., a damper constrained to the fixed space (Crosby and Karnopp 1973, Karnopp *et al.* 1974, Premount 2002). A conventional damper leads to resonance curves where for increasing values of damping the resonant response reduces, but this decrease is obtained only at the cost of an increased response for high frequencies. Sky hook dampers guarantee an overall response reduction at all frequencies and tend to cancel resonance.

The force in a real viscous damper is

$$F_v(t) = c_{real} \cdot \dot{x}_f(t) \tag{3}$$

whereas in a sky hook viscous damper it would be

$$F_v(t) = c_{sky} \cdot \left[\dot{x}_f(t) + \dot{x}_g(t)\right] \tag{4}$$

During a dynamic excitation of the device, a real damper can mimic a sky hook one if its constant c_{real} can vary so as the force expressed by Eq. (3) becomes equal to the one expressed by Eq. (4). However, the constant of a real damper cannot be set to a negative value and, therefore,

the control algorithm (herein referred to simply as "Sky Hook") has to be expressed as

$$\begin{aligned} &if \quad \frac{\dot{x}_f(t)+\dot{x}_g(t)}{\dot{x}_f(t)} \le 0 \quad then\ i(t)=i_{min}=0 \\ &if \quad \frac{\dot{x}_f(t)+\dot{x}_g(t)}{\dot{x}_f(t)} > 0 \quad then\ i(t)=i_{max} \end{aligned} \tag{5}$$

The 4th control algorithm tested was derived after a proposal of Stammers and Sireteanu (1998) related to the reduction of vibrations of industrial machines. The algorithm aims to minimize the amount of absolute accelerations in the main structure and, therefore, tries to minimize the energy transmission from the ground motion to the structure through the SA brace. By considering the global dynamic balance, reducing the sum of elastic and dissipative forces leads to the reduction of the inertial force, hence of the absolute acceleration of a given mass. The corresponding control algorithm (herein referred to as "Acceleration Reduction") imposes to take the device switched on if the elastic and dissipative forces have opposite signs (i.e., they tends to balance one each other), according to the following logic

$$\begin{aligned} &if \quad x_f(t)\cdot\left[\dot{x}_f(t)-\dot{x}_b(t)\right] > 0 \quad then\ i(t)=i_{min}=0 \\ &if \quad x_f(t)\cdot\left[\dot{x}_f(t)-\dot{x}_b(t)\right] \le 0 \quad then\ i(t)=i_{max} \end{aligned} \tag{6}$$

When not directly provided by the instruments installed, the quantities useful for the operation of the algorithms were derived from those measured. The velocities, in particular, are obtained by calculating on-line the derivatives of the displacements, to which a low pass filter (2nd order Butterworth with 60 Hz cutting frequency) has been applied.

Fig. 8 reports a zoom, for a time window of 0.5 second, of four tests done imposing at the base the same accelerogram (recorded along the North-South direction on 16/09/1978 by the station Tabas, Iran; its official identification code is "000187x", in the following often referred to simply as "187"; for the tests related to Fig. 8 the magnitude of accelerations was scaled at 50%) using each time a different algorithm. It also shows the measured command signal imposed by each control algorithm and reflecting the particular logic it is based on. As expected the Energy, Sky Hook and Acceleration Reduction algorithms apply a bi-state, on-off control policy that feeds the damper with a 0 or i_{max} current value. The MHF algorithm, conversely, is formulated to give, during the earthquake, also intermediate values of the current intensity (chosen in the interval [0, i_{max}] A). Nevertheless, from Fig. 8 it is shown that also on-off control strategies, that lead to sharp variations of the current and of the magnetic field (also thanks to the current driven command approach adopted), correspond to smooth variations of the force provided by a MR damper.

The 4 algorithms considered rely on measurement of displacement and/or velocities of the 1st floor relative to the base. As said above, velocities are calculated through numerical derivative of displacements. Therefore the issue of measuring displacements relative to the base arises. In the laboratory experiments, the problem has been easily solved by using a fixed reference structure. In realistic applications, laser measurements from a pole outside the building can be thought as a possible workaround, especially if the control devices and, in turn, the DOFs to be measured are located only at the lower floors, as in the experimental set up.

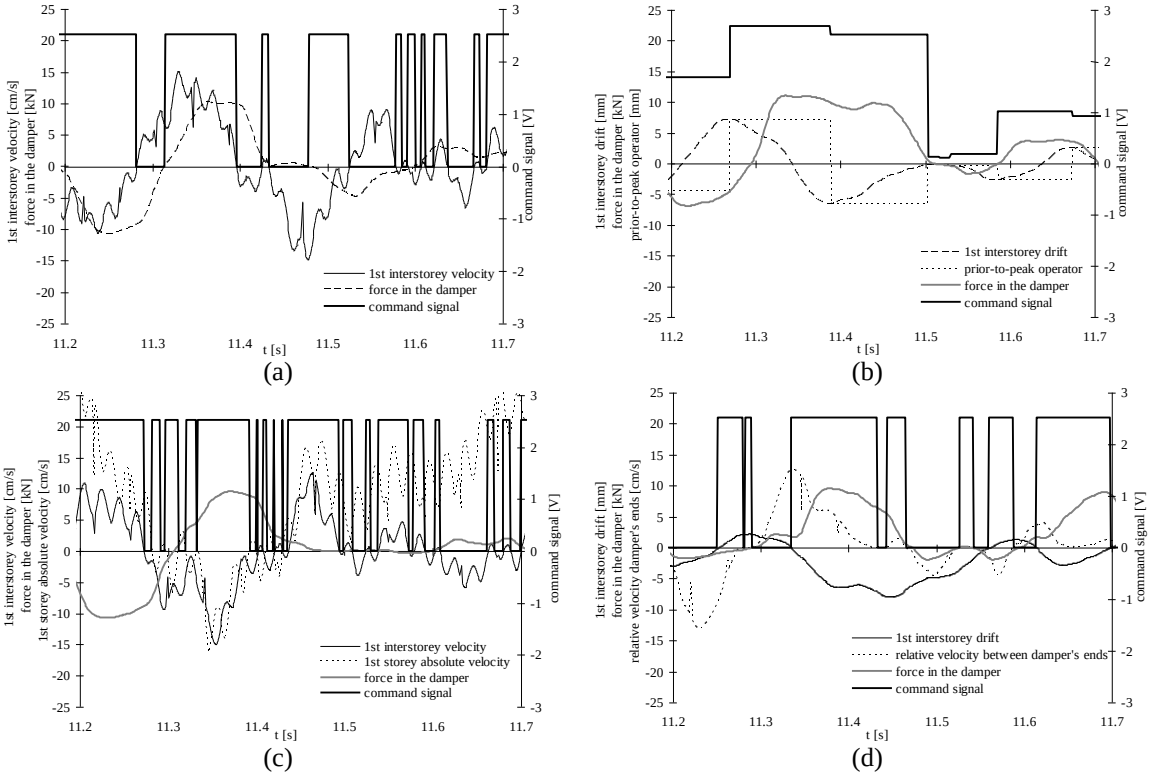

Fig. 8 An example of operation for each of the four control algorithm adopted for the tests: Energy (a), MHF (b), Sky Hook (c), Acceleration Reduction (d)

4. Experimental activity

The JETPACS steel structure mock-up has been dynamically tested commanding the actuator to move the frame in the longitudinal (X) direction, according to seven different natural records selected in the "European Strong Motion Database" and downloaded from the web site of the Italian network of university laboratories of seismic engineering RELUIS (http://www.reluis.it). They are characterized by a mean acceleration spectrum compatible with the elastic response spectrum of the Italian Seismic Code OPCM 3274 (2003) and of the Eurocode 8 (2005) for soil type B and seismic zone 1. The main characteristics of selected accelerograms are described in Tables 3 and 4.

The amplitude of the accelerations of earthquakes 000291y, 000535y, 001228x and 004673y has been multiplied by 1.5 in order to achieve the said spectral compatibility. Furthermore, the time scale of all accelerograms has been reduced by a factor $\sqrt{1.5}$ according to the scale of the model. The so obtained acceleration time-histories signals are in the following simply referred to as 187, 196, 291, 535, 1228, 4673 and 4677. Fig. 9 shows these 7 time-histories, modified as described, together with the superposition of the corresponding elastic acceleration spectra and the elastic response spectrum defined by the cited building code according to the parameters described above.

Seismic inputs have been applied at increasing amplitudes for subsequent tests, up to the achievement of a safety limit value for the interstorey drift (about 10 mm) or for the absolute floor acceleration (2 g). In particular, the following levels of seismic intensity have been considered: 25% (signal reduction of 75%), 50%, 75% and 100% (no reduction of seismic input), even if only for three of the seven earthquakes it has been possible to reproduce the 100% signal without going behind the above safety limits. Two records (187 and 535) have demonstrated to be particularly damaging for the structure, even for the lowest intensity level (25%).

The experimental activity comprised 50 SA valid tests. Table 5 shows their characteristics. A total of 23 tests has been performed using the Energy algorithm, involving all the seven acceleration records; 15 tests have been carried out imposing the MHF control logic, by applying the earthquake 535 in some cases, the 187 in others; 6 tests have been performed with the Sky Hook and Acceleration Reduction algorithms, under the same two types of seismic input at the base.

Table 3 Main characteristics of applied seismic inputs

Code	Direction	Magnitude	Fault distance [km]	PGA [g]
000187x	N-S	7.6	30	0.357
000196x	N-S	6.9	3	0.454
000291y	N279	6.6	1	0.769
000535y	N74E	7.3	8	0.926
001228x	E-W	6.9	13	0.264
004673y	TRAN	6.5	10	0.716
004677y	TRAN	6.5	20	0.227

Table 4 Identification of applied earthquakes

Code	Earthquake	Country	Date	Station
000187x	Tabas	Iran	16/09/1978	Tabas
000196x	Montenegro	Serbia	15/04/1979	Petrovac Hotel Oliva
000291y	Campano Lucano	Italy	23/11/1980	Calitri
000535y	Erzican	Turkey	13/03/1992	Erzican-Mudurlugu
001228x	Izmit	Turkey	17/08/1999	Gezbe-Tubitak Marmara Arastirma Merkezi
004673y	South Iceland	Iceland	17/06/2000	Hella
004677y	South Iceland	Iceland	17/06/2000	Selsund

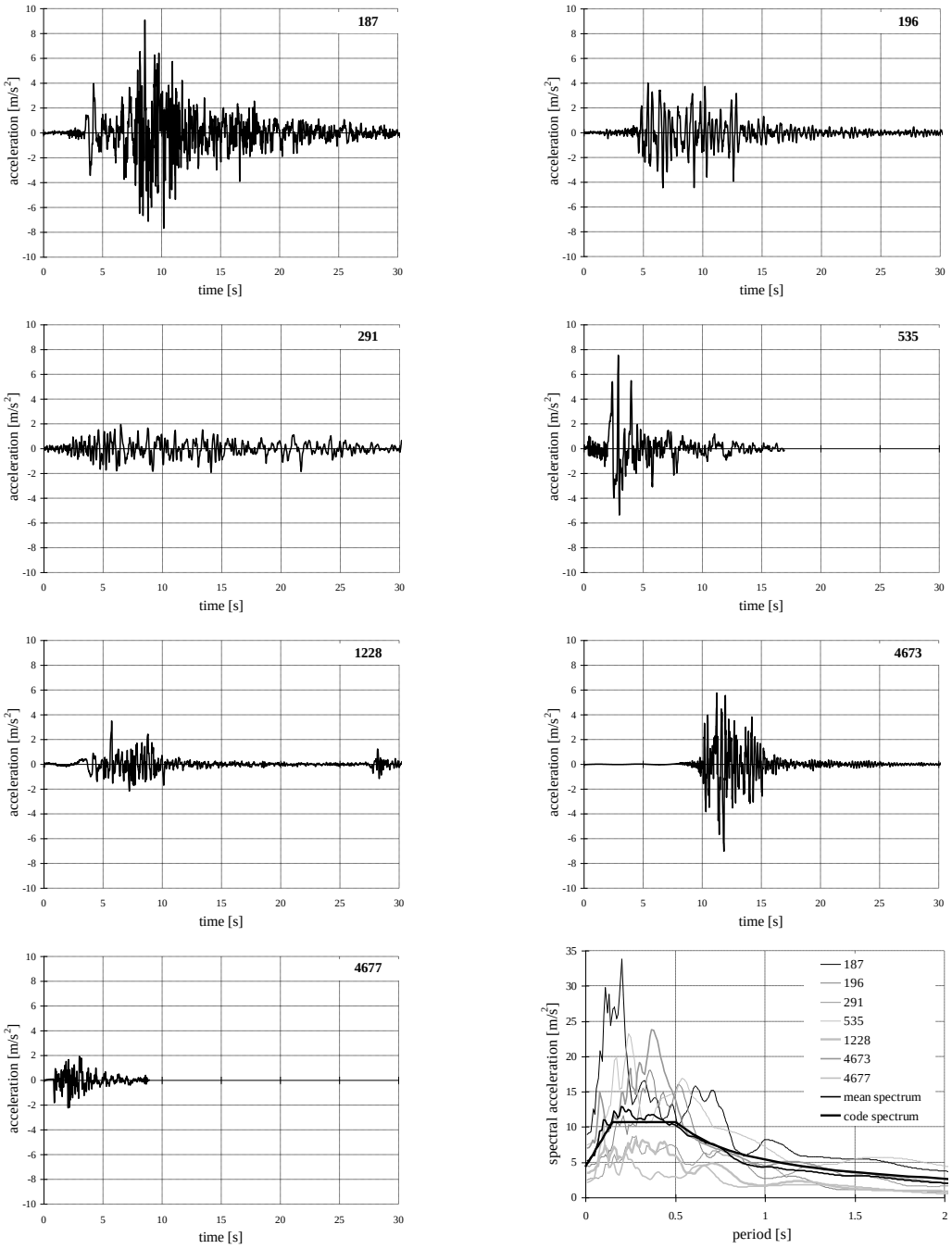

Fig. 9 Time-histories and elastic acceleration spectra (5% damping) of seismic inputs

Table 5 Experimental activity

Accelerogram	Input level [%]	Control algorithm	Max. current [A]	Type of connection
187	50	Energy	1.0	Flexible
187	25, 50	MHF	1.5, 2.5	Rigid
187	25, 50	Sky Hook	1.0, 2.5	Rigid
187	25, 50	Acc. Red.	1.0, 2.0	Rigid
196	25, 50, 75	Energy	1.0, 2.5	Flexible
291	50, 100	Energy	1.0	Flexible
535	25, 50, 75	Energy	1.0, 1.5, 2.0, 2.5	Flexible
535	25	MHF	1.5, 2.5	Rigid
535	25	Sky Hook	1.0, 2.0	Rigid
535	25	Acc. Red.	1.0, 2.0	Rigid
1228	10, 25, 50, 75, 100	Energy	1.0, 2.5	Flexible
4673	50	Energy	1.0	Flexible
4677	50, 100	Energy	1.0	Flexible

All the four control logics have been tested under the action of the heaviest earthquakes (187 and 535) allowing the effective comparison described in the following. The effectiveness of each control logic for a given earthquake at a certain input level has been also investigated repeating the same test with different values of imposed maximum intensity of current i_{max}. Table 5 (last column) also shows the type of connection of MR dampers to the chevron-type braces (flexible or rigid; ref. Section 2.2, Fig. 5) adopted for each test. It depended on the algorithm: the algorithm Energy requires a flexible connection (whose stiffness has been calibrated for this purpose) in order to work as described before (i.e., to store strain energy in selected intervals of time), whereas the other control algorithms turned out to be more effective with a rigid link.

5. Operations and failures of control algorithms

Control malfunctions may happen during SA tests: depending on many factors, it is possible that, in certain instants of the test, the electronic system described above is not able to take the right decision (i.e., the one that would derive from the correct application of the control logic) or to turn it in the right command to the power supplier. If the control system is properly designed, these failures have a low incidence (i.e., occur only in a few instants of the motion) and could generally be neglected. However, according to the results of 3 different laboratory experiences (Occhiuzzi and Serino, 2003 and Occhiuzzi and Spizzuoco 2005), failures of the control system cannot be excluded *a priori*. In earthquake engineering even a single failure may correspond to big losses, both in terms of human life and from an economical perspective. Therefore, control algorithms yielding minimum failure rates should be preferred.

Table 6 Percentage of wrong operations to the total number of theoretical control operations

Control algorithm	Failures	During the strong motion
Energy	6.48 %	3.33 %
MHF	0.02 %	0.03 %
Sky Hook	0.03 %	0.03 %
Acc. Red.	0.06 %	0.02 %

For each of the above described 50 dynamic experimental tests, all the time instants corresponding to a wrong operation of the control system have been singled out by manual inspection of the files, checking when the command signal to the devices did not provide the control required by the analytical formulation of the algorithm. Then, the duration of the strong ground motion (Bolt 1969) has been evaluated for each applied seismic input as the time interval between the first and the last peak acceleration over $0.2g$ for the heavier earthquakes and over $0.1g$ for the other ones, and the number of wrong operations falling in the strong motion time interval has also been manually counted.

Table 6 reports the maximum value, computed on all the tests performed by applying the same control algorithm, of the percentage of undesired operations to the total number of theoretical control operations for the whole duration of the test and for the duration of strong motion only. The table makes clear that malfunctions assumed a quite significant incidence only for the tests driven according to the "Energy" control logic, whereas they resulted to be negligible in the other tests.

Wrong operations registered during the tests driven by MHF, Sky Hook and Acceleration Reduction algorithms actually involved a maximum control delay bounded to one millisecond at a time, i.e., to a single time step. Therefore they had not any influence on the efficacy of the control systems, since this little amount of time is not enough to make the force in the damper actually change. However, figures in Table 6 help understanding how the theoretical effectiveness of a control algorithm may be endangered by the number and the quality of on-line measurement and processing.

In the case of Energy algorithm, we observed similar delays, but also some more severe misoperations of the control system. Fig. 10 shows a 50 ms time window of the test No. 11 (535 accelerogram scaled at 75% of its actual amplitude) with the Energy algorithm set to a maximum current value of 1 A. The Figure allows to discuss in a more general way three different behavior the control system exhibited during the tests:

1. Almost always the given command signal was coincident with the desired one (see white arrows in the figure).
2. Sometimes, the registered command voltage followed the desired command by just 1 ms (see gray arrows in figure). This type of delay is considered not severe, since sometimes (for indeterminable reasons) calculations slightly slowed down, requiring an additional time step (just 1 ms, given the 1 kHz sampling rate) to be completed and to send a command signal to the power supply.

3. Other times (black arrows in figure) the given command signal more evidently deviated from the desired one, even for longer time intervals. This kind of failures (missed command to the damper), if located in the strong phase of the earthquake, may lead to undesired peak response of the structure. In other words, the reliability of the control system is a critical issue in seismic applications of SA structural control and, from this perspective, simple and model-free control algorithms should be preferred.

It is worth noting that the synthetic data reported in Table 6 accounts for each kind of detected differences between registered and desired command signal (i.e., both types 2 and 3 above), for each algorithm, but severe failures are only those described on item 3 of the list above.

All the adopted algorithms are such that they change the command signal each time a given function of the time changes its sign, i.e., it passes from zero. Being the equipment the same in all tests, only the Energy algorithms requires measurement of forces in addition to measurement of displacements. The higher incidence of malfunctions on the tests driven by the Energy algorithm, in comparison to the other algorithms, could be motivated noting that only Energy uses, as reference for deciding the command signal, the product of two quantities, i.e., force and velocities, different in nature and measured by transducers based on quite different physical principles and manufactured with different technologies. Processing such different signals causes unexpected and unpredictable "black-outs" on data processing.

6. Reduction of structural response

Control algorithms are herein compared in terms of interstorey drift demand as well as of floor response spectra (FRS), the latter being strongly related to non-structural components and contents demand (Sackman and Kelly 1979).

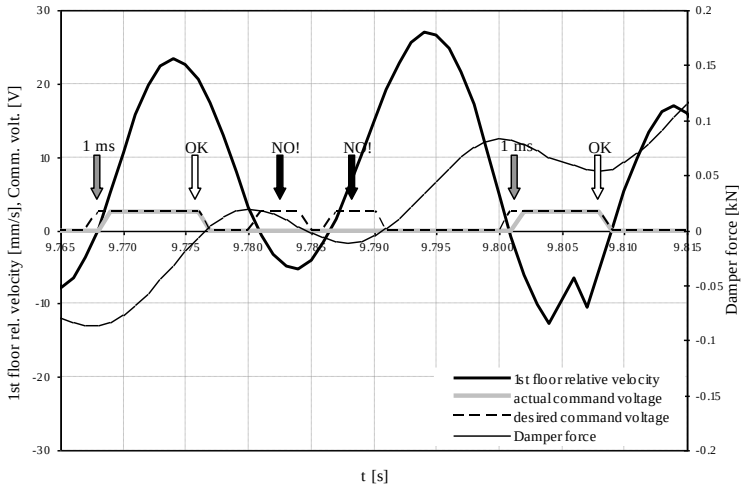

Fig. 10 535-75% earthquake: right and wrong operations by Energy algorithm

Table 7 Peak interstorey drifts under 187-50% and 535-25% earthquake: comparison of algorithms

Earthquake	Test #	Algorithm	i_{max} [A]	0-1 drift [mm]	1-2 drift [mm]
187-50%	12	Energy	1.0	6.00	10.88
	30	MHF	1.5	7.36	10.38
	36	Sky Hook	1.0	6.80	9.02
	41	Accel. Reduction	2.0	7.03	9.01
535-25%	-	*Uncontrolled*	-	*6.01*	*7.94*
	4	Energy	2.5	5.49	10.88
	27	MHF	2.5	6.16	9.22
	37	Sky Hook	1.0	3.22	4.68
	43	Accel. Reduction	1.0	4.98	5.86

All the tests have been analyzed in terms of displacements and accelerations, even if the most interesting results comes from tests performed using the 187 and 535 accelerograms scaled at 50% and 25%, respectively. For this reason the comparison will be focused on them. In particular, the results of the tests under the 535-25% signal are available for all of the algorithms, set to different values of current intensities, and for the bare structure, i.e. the frame without any damping device or brace, which is referred to as the "uncontrolled" structure. Comparison between the uncontrolled structure and the various algorithms considered corresponds to the comparison of a structure before retrofitting and different seismic upgrade methods. Authors regret not to have data about "passive on" or "passive off" control configurations, due to time restraints in the use of the testing facility.

6.1 Comparison of algorithms in terms of interstorey drift

For each algorithm, the maximum value i_{max} of the current feeding the MR dampers could be selected in the range 1.0÷2.5 A, corresponding to command signals issued to the power supply in the range 2.5÷6.3 V, as the gain of the power supply is about 2.5 V/A (input over output). In principle, the best value of i_{max} does not necessarily is the same for each control algorithm. In the comparison, for each algorithm the current intensity corresponding to the greater reduction of drifts (i.e., the one leading to the better performance of the given control logic), when different values were available, has been selected. Table 7 reports the corresponding peak interstorey drifts, whereas Fig. 11 graphically represents the same data.

The experimental data confirm that drift reduction achieved by SA control system, compared to the bare, uncontrolled frame, can be close to 50% (sky-hook algorithm, 0-1 drift, 535-25% seismic input), as often reported in the scientific literature based on numerical analyses. However, the response reduction provided by a SA control system can also be negligible, or even negative, depending on the amount of misoperations of the control algorithm adopted which, in turn, are directly related to its complexity.

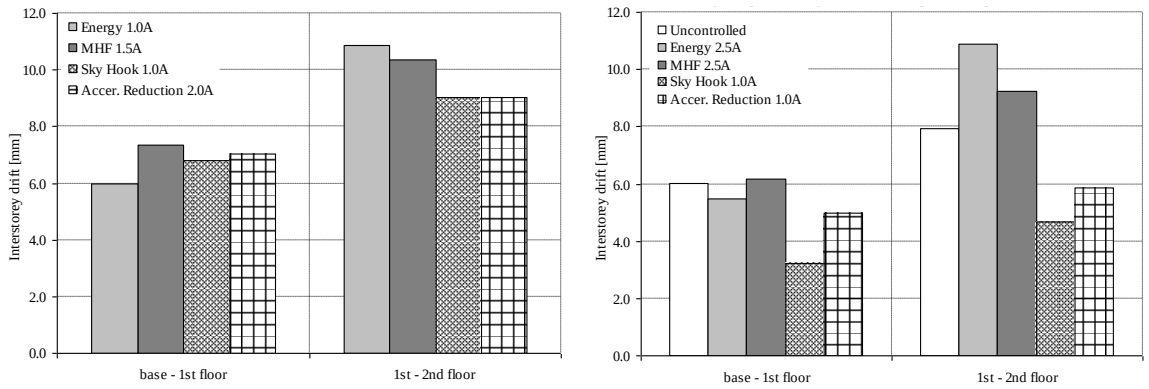

Fig. 11 Comparison of algorithms in terms of peak interstorey drift demand: 187-50% (left), 535-25% (right) earthquakes

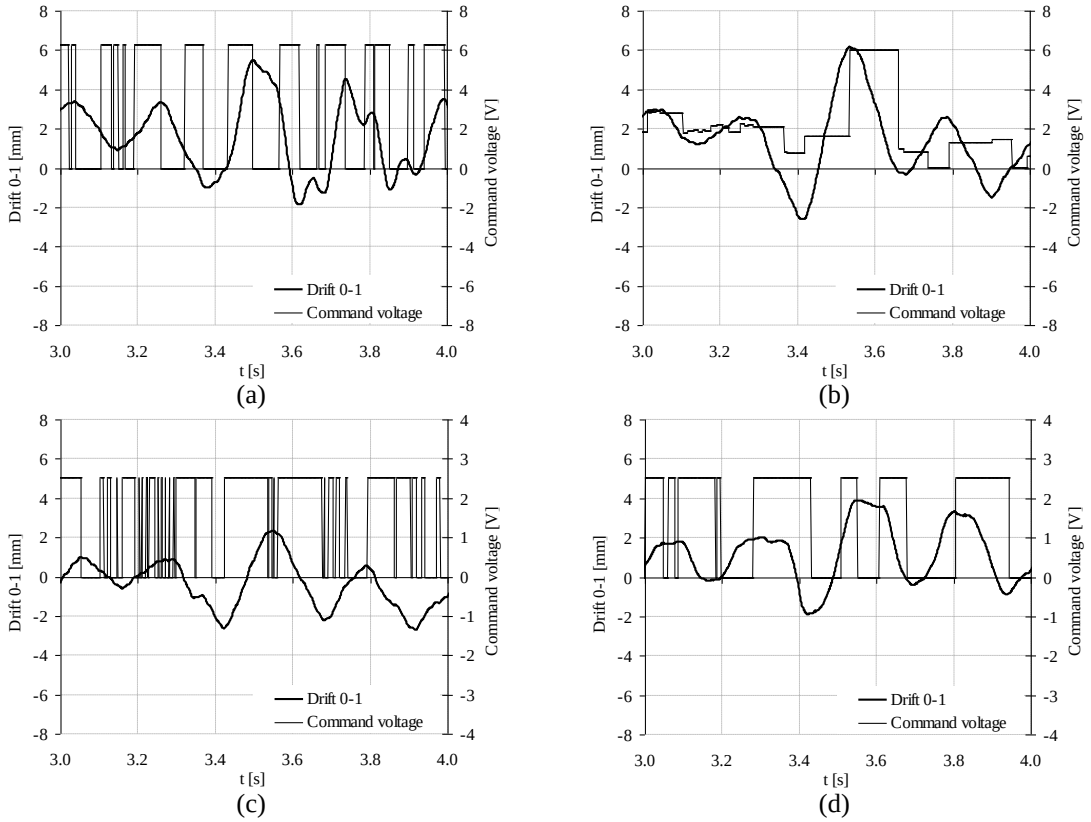

Fig. 12 1st interstorey drift and command signal for a 1 second time window under the 535-25% earthquake and using the algorithms Energy-2.5A (a), MHF-2.5A (b), Sky Hook-1.0A (c), Acc. Reduction-1.0A

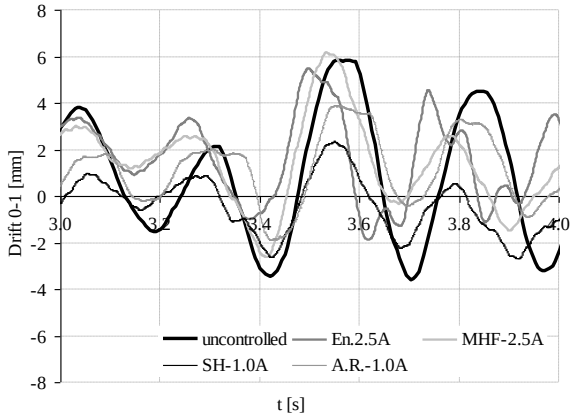

Fig. 13 1st interstorey drift response for a 1 second time window under the 535-25% earthquake: comparison of uncontrolled and SA controlled cases

With reference to the 535-25% earthquake, Fig. 12 shows the 1st interstorey drift response and the command signal for each algorithm, during a 1 second time window corresponding to the most severe portion of the input motion. Finally, Fig. 13 reports, for the same time window, the superposition of said interstorey drifts and the one relative to the uncontrolled structure.

One can first observe the very different behavior of the control algorithms. Fig. 12 highlights, for the same input motion and the same time window, how different is the command signal each control logic imposed.

As far bang-bang algorithms are concerned (all but MHF), one can notice that Sky Hook causes the largest number of change of status (on to off and *vice versa*), sometimes the latter being separated by only a few milliseconds. During the zoomed time interval, the device is held on for the greatest number of moments. Conversely, the Energy algorithm seems to be more regular, imposing alternate phases of on and off, of comparable duration. The lowest number of changes of status is registered when the Acceleration Reduction algorithm was adopted, generally being spaced out by dozen of milliseconds.

Completely different is the behavior of the MHF algorithm, where the command voltage may vary from zero to the maximum set value according (proportionally) to the magnitude of the last peak of 1st interstorey drift (absolute value), being calibrated so that the maximum allowable value for the 1st interstorey drift corresponds to the maximum command voltage.

As a consequence, also the trend and the amplitude of the interstorey drift at the 1st floor resulted to be very different. Fig. 13 shows the plot of these signal over the above time window, allowing a comparison of algorithms in terms of effectiveness, consistently with what already observed with reference to the peak values of the drift (Fig. 11, right).

Some remarks have to be given about the interstorey drift at the 2nd floor and the ability of control algorithms to manage it, also considering that neither measurements to be adopted in the control algorithms nor control forces existed at that floor. From Fig. 11 one can observe that the 1-2 drift is often relatively large, sometimes overcoming the one corresponding to the uncontrolled structure. This can be explained as follows

- the presence of dampers only at the first floor of the building introduces an irregular

distribution of damping over the height of the structure that affects the mode shapes;

- for the same reason the control system has little chances of actually control the drift at the second floor, that may strongly rise especially when the control forces excite, with their predominant frequencies, the second vibration mode of the structure.

For the test No. 4, done with the Energy algorithm and the earthquake 535 at 25%, Fig. 14 shows the Fourier spectrum of the West damper's force. It is possible to notice that this signal is characterized by a significant harmonic at 12.15 Hz, quite close to the second natural frequency of the structure (Table 1).

This kind of spillover effect would have been hardly noticeable if SA MR dampers would be mounted at the 2nd floor of the tested structure, too. Even if reactive devices are not able to input energy into the hosting structure, their effect can, in principle, emphasize resonance (Preumont 2002). Therefore, differently from passive control systems, SA devices located only at few DOFs of a structure can increase the structural response at uncontrolled DOFs.

6.2 Comparison of algorithms in terms of accelerations

All the tests performed with earthquakes 187-50% and 535-25% have been analyzed also in terms of floor accelerations. For each algorithm, the optimal value of the current intensity i_{max}, i.e., the one corresponding to minimum accelerations, resulted to be coincident with those already found about the control of drifts (187-50%: 1.0A for Energy, Sky Hook, 1.5A for MHF, 2.0A for Acceleration Reduction; 535-25%: 2.5A for Energy and MHF, 1.0A for Sky Hook and Acceleration Reduction).

Fig. 15 shows the response of both floors under the action of the 535-25% earthquake and allows to compare the acceleration time histories for the uncontrolled and controlled (by the four control logics) configurations. All the controllers have been able to significantly reduce the acceleration demand. Only in one case (Energy algorithm, 1st floor) the controller has not appreciably reduced the peak floor acceleration, even if the cyclic demand over the entire duration of the earthquake has been highly damped in respect to the uncontrolled condition. MHF and Sky Hook algorithms showed the best results in terms of acceleration control.

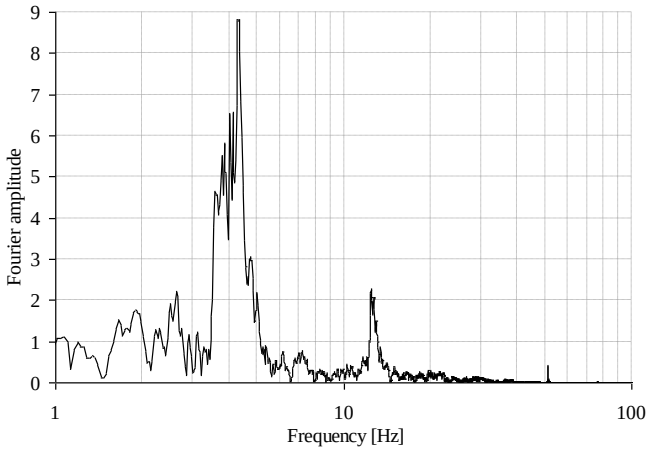

Fig. 14 Fourier spectrum of the West damper's force during the test No. 4 (Energy, 535-25% earthquake)

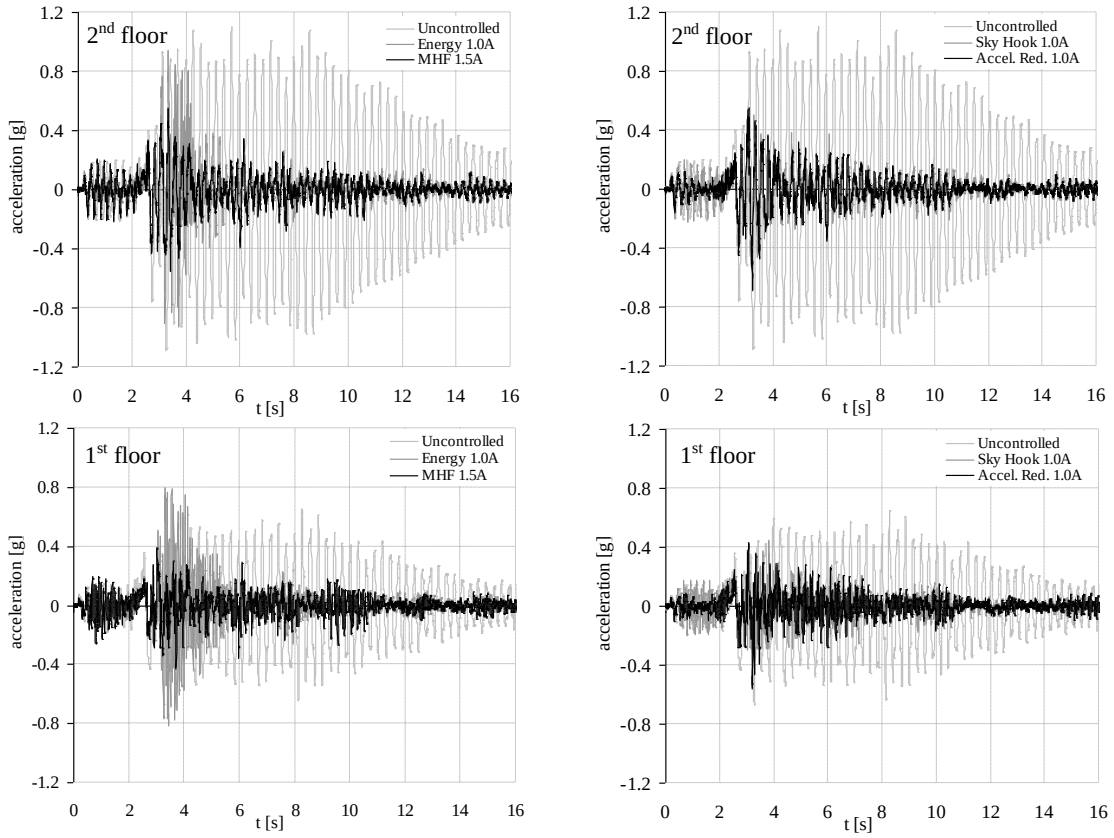

Fig. 15 Absolute acceleration for the 535-25% earthquake: comparison of the uncontrolled and controlled responses

Furthermore, floor response spectra (FRS) were referenced and utilized in the following as a effective tool to analyze, from a different point of view, how the controllers affected absolute acceleration response. Similarly to earthquake response spectra, FRS summarize the peak response in terms of acceleration of a single degree of freedom system attached on a given floor (rather than on the moving ground) when the frequency (or, correspondingly, the natural period) of the system varies in the range of interest. FRS are the most appropriate measure of the seismic demand for non-structural components and contents (Sackman and Kelly 1979).

Fig. 16 shows the floor response spectra for the tests assumed as reference for comparison. The parts (a) and (b) refer to the tests under the 187-50% signal, the other parts (c) and (d) to those performed imposing the 535-25% accelerogram. As before, the latter parts (535-25%) allow to draw more comments, because they include measurements of the uncontrolled structure. These diagrams should be read in this sense: given a non-structural component having elastic period T_{ns}, each diagram reports the maximum absolute acceleration of such element during the earthquake. T_{ns} close to zero stands for components rigidly connected to the structure; higher values of T_{ns} correspond to non-structural elements linked in a more flexible way to the hosting frame. The results shown can be analyzed at three characteristic parts of such diagrams: 1) T_{ns} close to zero (rigidly connected element); 2) T_{ns} around the first natural period of the structure (0.280 s); 3) T_{ns}

around the second natural period of the structure (0.081 s). The following comments can be drawn:

- no significant differences can be highlighted around the part 1) of the different curves belonging to the same diagram: different algorithms seem to produce very similar effects in terms of acceleration induced on components firmly connected to the structure;
- by looking at the diagram (c), the 1st floor spectral acceleration for $T_{ns} \approx 0$ registered for the uncontrolled structure seems to be substantially unchanged when a SA control strategy is considered, whatever algorithm is considered;
- as the diagram (d) is concerned, a reduction of the spectral acceleration of the 2nd floor for $T_{ns} \approx 0$ can be observed when a control strategy is adopted, this reduction varying from almost 50% (Sky Hook algorithm) to about 75% (Energy);
- some differences among floor response spectra corresponding to different algorithms can be observed for values of T_{ns} greater than zero, even if these seem to be negligible with the single exception discussed in the following;

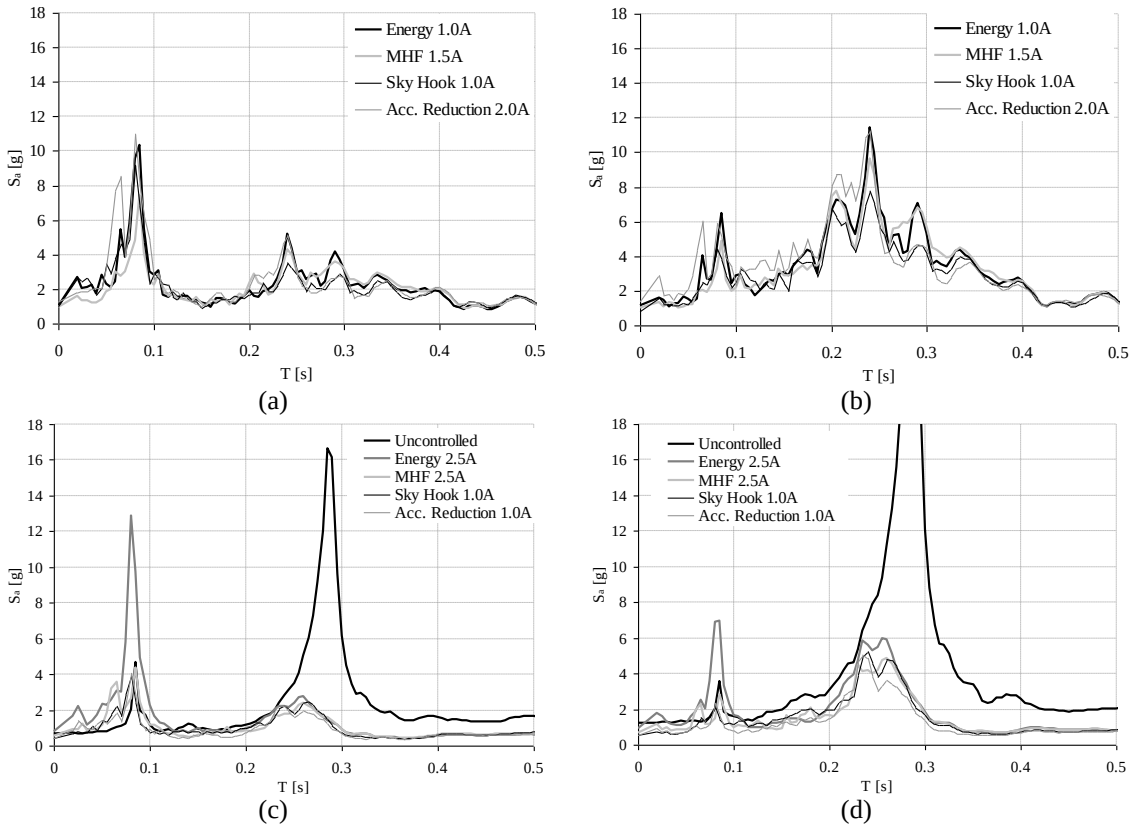

Fig. 16 Floor response spectra and comparison of algorithms: earthquake 187-50%, 1st floor (a) and 2nd floor (b); earthquake 535-25%, 1st floor (c) and 2nd floor (d)

- by comparing the 5 curves of diagrams (c) and (d) one can observe that all the control algorithms lead to a drastic reduction of the floor spectral acceleration in the zone 2) in respect to

the uncontrolled condition, both at the 1st and the 2nd floor; the same algorithms result to be much less effective in terms of mitigation of floor acceleration in the period zone 3), often leading to almost the same values of the uncontrolled structure;

- in the field of period 3) the Energy algorithm causes an increase of floor accelerations in respect to the uncontrolled conditions; this undesired effect is related a) to the absence of SA devices at the 2nd floor (i.e., the above discussed inability of the system of controlling the 2nd mode of vibration), b) to the fact that during this test the control forces exerted by the MR dampers excited, with their predominant frequency content, just the 2nd mode of the structure (spill over effect).

7. Dissipative capabilities

The behaviour of the frame structure equipped with the SA bracing control systems can be observed from the energy balance perspective, described in Eq. (7).

$$E_{el}(t) + E_{kin}(t) + E_{diss}(t) = E_{inp}(t) \tag{7}$$

where:

- $E_{el}(t) = 0.5\ \mathbf{x}^T(t)\ \mathbf{K}\ \mathbf{x}(t)$ is the elastic stored energy at the time t;
- $E_{kin}(t) = 0.5\ \dot{\mathbf{x}}_t^T(t)\ \mathbf{M}\ \dot{\mathbf{x}}_t(t)$ is the absolute kinetic energy at the time t;
- $E_{inp}(t)$ is the seismic input energy, equal to the product $\ddot{\mathbf{x}}_t^T(t)\ \mathbf{M}\ \mathbf{i}\ \mathrm{d}x_g(t)$ integrated from the initial instant up to the current time t;
- $E_{diss}(t)$ is the dissipated energy, obtained by difference through Eq. (7).
- **M** and **K** are the mass and stiffness matrices of the structure, respectively;
- $\ddot{\mathbf{x}}$, $\dot{\mathbf{x}}$, and **x** are the accelerations, velocities and displacements vectors relative to the base;
- $\ddot{x}_g$ is the acceleration at the base of the structure;
- **i** is a column vector with all elements equal to 1;
- $\ddot{\mathbf{x}}_t$ is the absolute accelerations vector, equal to $\ddot{\mathbf{x}} + \mathbf{i}\,\ddot{x}_g$;

The masses (expressed in tons) and stiffnesses (in kN/m) matrices of the dynamic system are reported in Eq. (8), in the case of absence of stiffening steel plates (Fig. 5(b)). These matrices are referred to a 2+1 DOFs model considering the masses of the two floors and that of the SA brace and assuming that only displacements along the X axis of these masses are allowed. They have been calibrated according to available experimental data relative to the frame in uncontrolled conditions (Table 1).

$$\mathbf{M} = \begin{bmatrix} 4.768 & 0 & 0 \\ 0 & 4.560 & 0 \\ 0 & 0 & 0.032 \end{bmatrix}; \qquad \mathbf{K} = \begin{bmatrix} 21508 & -10017 & 0 \\ -10017 & 7395 & 0 \\ 0 & 0 & 20408 \end{bmatrix} \tag{8}$$

Due to the moderate values of the inherent structural damping ratios identified for the bare steel frame (Table 1), the whole energy dissipation is considered associated to the SA devices.

All the performed tests have been analyzed in terms of energy balance, even if the most interesting results (as for drifts and floor accelerations) comes from tests done using the 187 and 535 accelerograms scaled at 50% and 25% respectively. In particular, the instantaneous, final and maximum value of each one of the above energies have been computed in order to define, for each algorithm, the optimal value of the maximum current intensity i_{max}, i.e., the value corresponding to

the minimum energy demand in the structure (the sum of elastic and kinetic energies is assumed as a measure of this demand). These values resulted to be coincident with those already found with reference to drifts and floor accelerations (187-50%: 1.0A for Energy and Sky Hook, 1.5A for MHF, 2.0A for Acceleration Reduction; 535-25%: 2.5A for Energy and MHF, 1.0A for Sky Hook and Acceleration Reduction), allowing to conclude that, for given seismic input, the optimal calibration of each algorithm can be univocally defined.

Figs. 17 and 18 show the input energy and the sum of elastic and kinetic energies over the time for 4 tests done with the 187-50% accelerogram (one for each control algorithm) and 5 tests done with the 535-25% signal (one for each algorithm plus the uncontrolled conditions). Tables 8 and 9 summarize some results of these analysis, reporting for each test maximum values of the input energy and of the sum of elastic and kinetic energies. The tables also describe the relative frequency of occurrence of energy values falling into each of four predefined interval of values. This frequency has been evaluated as the ratio of the sum of the time intervals where the $E_{el} + E_{kin}$ falls into one of the intervals over the whole test duration.

The total input energy corresponding to a given earthquake (187-50% or 535-25%) resulted to be strongly dependent on the control algorithm adopted, allowing to highlight how SA control via MR dampers is able to modify the global dynamic properties of the hosting structural system. In the two investigated cases, the Energy algorithm yields the biggest amount of input energy, the Sky Hook logic the smallest one. This behaviour seem consistent with results in terms of drift and floor acceleration spectra shown in the previous section.

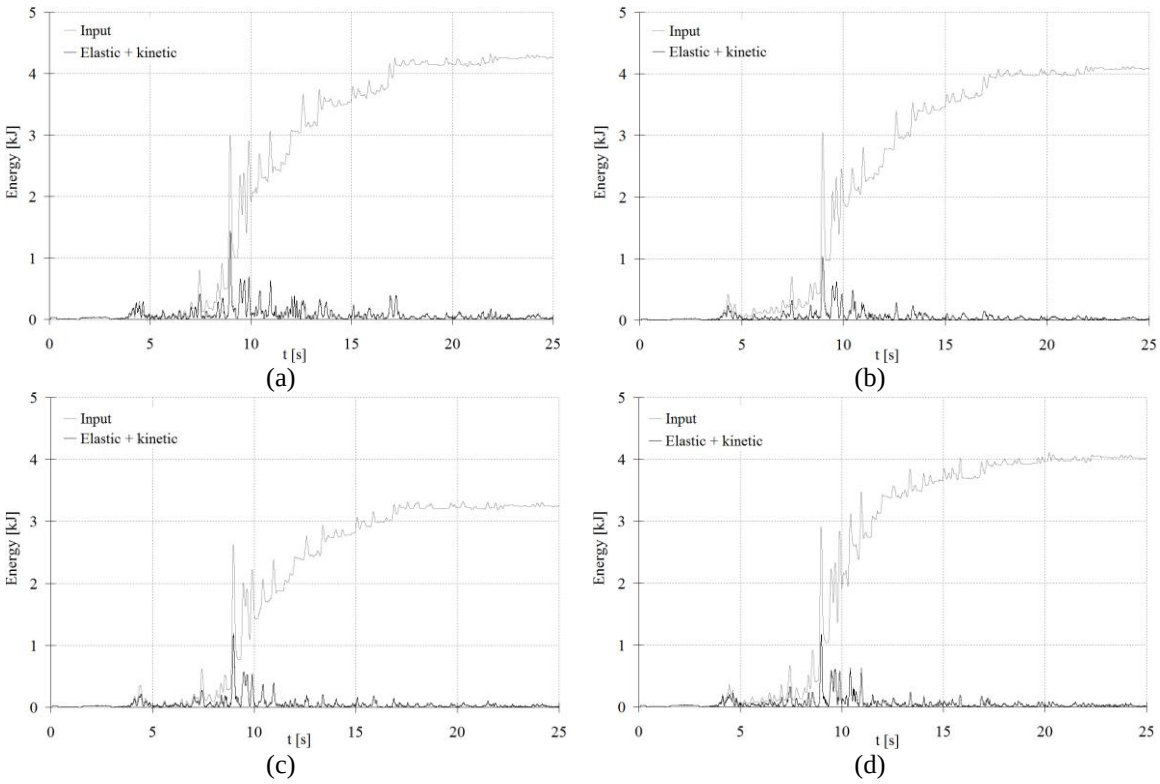

Fig. 17 Comparison of energies due to 187_50% earthquake, for different algorithms: (a) Energy, (b) MHF, (c) SkyHook, (d) Acceleration Reduction

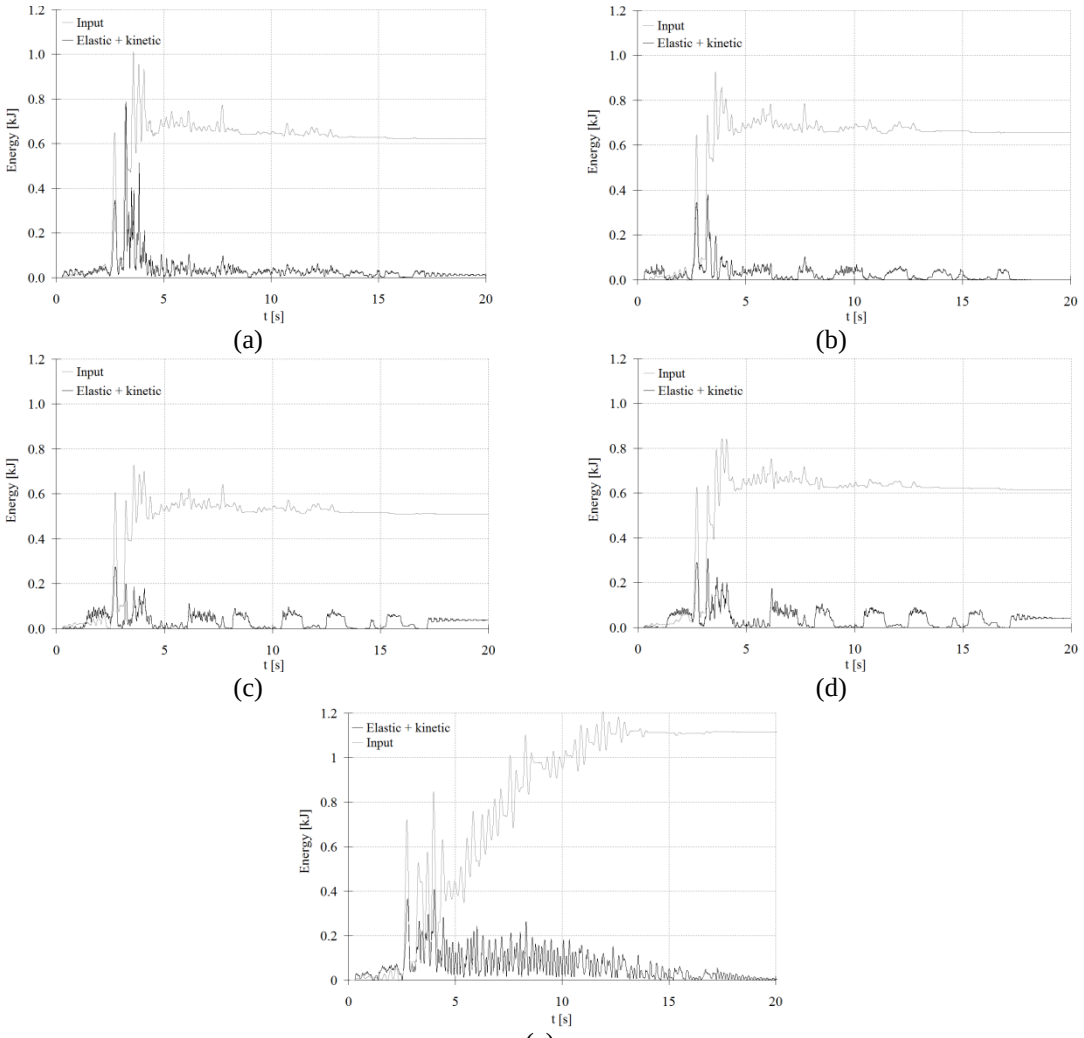

Fig. 18 Comparison of energies due to 535-25% earthquake, for different algorithms: (a) Energy, (b) MHF, (c) SkyHook, (d) Acceleration Reduction, (e) Uncontrolled structure

Table 8 Energy analysis referred to 4 tests done with earthquake 187-50%

Control algorithm	max(E_{inp}) [kJ]	max(E_{el} + E_{kin}) [kJ]	Occurrence of values E_{el} + E_{kin} within given intervals of magnitude [kJ]			
			0.0-0.1	0.1-0.5	0.5-1.0	1.0-1.5
Energy	4.32	1.44	79.2%	19.3%	1.2%	0.3%
MHF	4.13	1.03	87.5%	11.6%	0.8%	0.1%
Sky Hook	3.32	1.19	89.5%	9.4%	0.9%	0.2%
Accel. Reduct.	4.11	1.18	86.5%	12.0%	1.3%	0.2%

Table 9 Energy analysis referred to 5 tests done with earthquake 535-25%

Control algorithm	max(E_{inp}) [kJ]	max(E_{el} + E_{kin}) [kJ]	Occurrence of values E_{el} + E_{kin} within given intervals of magnitude [kJ]			
			0.00-0.05	0.05-0.10	0.10-0.15	0.15-0.80
Energy	1.01	0.79	87.6%	7.5%	1.1%	3.8%
MHF	0.93	0.38	87.4%	9.9%	0.7%	2.0%
Sky Hook	0.73	0.28	70.6%	26.3%	1.7%	1.4%
Accel. Reduct.	0.84	0.31	64.9%	29.7%	2.6%	2.8%
Uncontrolled	1.21	*0.41*	*53.5%*	*22.5%*	*13.8%*	*10.2%*

By considering the sum of elastic and kinetic energies (assumed as a measure of the structural demand), the analysis of the results of the tests done with the 187-50% signal yields the following comments:

- the maximum value of E_{el} + E_{kin} varies according to the adopted control logic, and assumes the biggest value for Energy, intermediate values for Acceleration reduction and Sky Hook, the smallest value for MHF;
- almost all the values of E_{el} + E_{kin} fall in the range 0.0-0.5 kJ for all the 4 tests, even if the Energy algorithm corresponds to a larger occurrence of values in the upper part of this interval; conversely, the Sky Hook algorithm gives about the 90% of E_{el} + E_{kin} values in the range 0.0-0.1 kJ, thus showing a peculiar capacity of manage the strongest part of the seismic input .

Similar comments can be repeated for the tests performed with the 535-25% earthquake, with the further possibility to include in the comparison the uncontrolled case:

- the maximum value of E_{el} + E_{kin} evaluated for each SA test again assumes the biggest value for the Energy algorithm, even greater than the one corresponding to the uncontrolled case, highlighting a poor performance of the algorithm in this case (see also section 5); from this perspective the Sky Hook algorithms yielded the better performances;
- all of the tested algorithms was able to bound the big majority of E_{el} + E_{kin} values in the range 0.00-0.15 kJ, thus decreasing the number of strong cycles compared to the uncontrolled case; again, the Energy and Sky Hook algorithms corresponded to the worse and best response reduction.

8. Effectiveness of control algorithms through indexes

Starting from the results shown in the previous sections, the effectiveness of the four investigated control logics has been also verified through six properly defined evaluation criteria related to the structural response and to the required performance of the control devices. The criteria, similar to those proposed in literature (Ohtori *et al.* 2004), are characterized by a "the smaller the value, the better the performance" fashion. Values greater than 1 denotes a response worse than the corresponding uncontrolled case.

The six criteria are described in Eq. (9). Due to the need of the uncontrolled response, they could only be applied to tests under the 535-25% earthquake.

$$I_1 = \frac{\max_t \left| d_{c,1}(t) \right|}{\max_t \left| d_{unc,1}(t) \right|} \qquad I_2 = \frac{\max_t \left| d_{c,2}(t) \right|}{\max_t \left| d_{unc,2}(t) \right|} \qquad I_3 = \frac{\max_t \left| \sum_i m_i \ddot{x}_{tot,i}(t) \right|}{\max_t \left| F_{b,unc} \right|}$$

$$I_4 = \frac{\max_{t,i} \left| f_i(t) \right|}{W} \qquad I_5 = \frac{\max_{t,i} \left| \Delta_i(t) \right|}{\max_t \left| d_{unc,1}(t) \right|} \qquad I_6 = \frac{\max_t \left| E_{el}(t) + E_{kin}(t) \right|_c}{\max_t \left| E_{el}(t) + E_{kin}(t) \right|_{unc}} \tag{9}$$

- I_1 is determined singling out the maximum peak interstorey drift ($max \mid d_{1,c} \mid$) of the 1st floor and dividing it by the homologous value relative to the uncontrolled structure ($max \mid d_{unc,1} \mid$).
- I_2 is defined as I_1 but referred to the 2nd storey;
- I_3 is defined as the ratio between the maximum value of the base shear registered during a SA test and the one ($max \mid F_{b,unc} \mid$) obtained by the uncontrolled test; m_i is the seismic mass of the i-th floor, $\ddot{x}_{tot,i}$ its absolute acceleration;
- I_4 is the maximum control force exhibited by the two MR devices normalized by the seismic weight W of the building (f_i is the force in the i-th device, with i = 1, 2);
- I_5 is the maximum stroke Δ_i of the i-th control device (i = 1, 2) normalized by the maximum 1st interstorey drift of the uncontrolled test;
- I_6 is the maximum value of the sum of elastic and kinetic energies normalized by the homologous value relative to the uncontrolled case.

Fig. 19 graphically summarizes the results of the index analysis, allowing a direct comparison among different algorithms' effects on structural response.

Almost for all the assumed criteria, the Energy algorithm leaded to the worst performances, Sky Hook to the best ones, but, again, misoperations of the control systems had a strong role in these results. Also the Acceleration Reduction algorithm determined a significant reduction of the structural response together with a fair behaviour of the control devices.

Table 10 Evaluation indexes for the JETPACS structure under the 535-25% earthquake

Performance index		Control algorithm			
		Energy	MHF	Sky Hook	Acc. Red.
I_1	(1st interstorey drift)	0.913	1.024	**0.535**	0.829
I_2	(2nd interstorey drift)	1.371	1.162	**0.590**	0.739
I_3	(base shear)	1.549	1.111	**0.967**	1.071
I_4	(control force)	0.241	0.226	**0.127**	0.136
I_5	(control device stroke)	0.644	0.695	**0.478**	0.657
I_6	(elastic + kinetic energies)	1.928	0.937	**0.674**	0.755

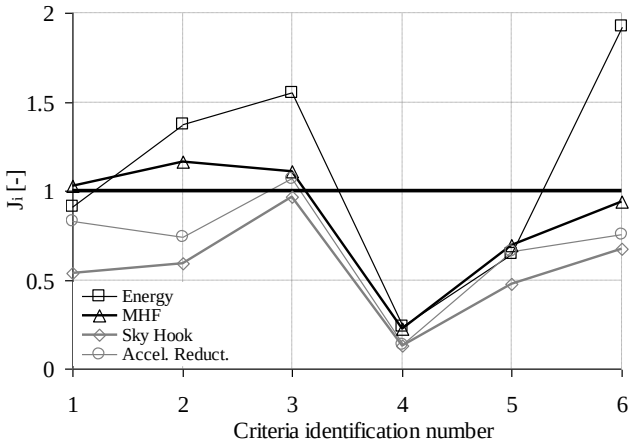

Fig. 19 Performance indexes according to the 4 control algorithms (tests with 535-25% earthquake)

9. Conclusions

The main results of a wide experimental campaign on a near full-scale semi-actively controlled steel building have been presented and discussed (data are available to the reader via the following download www.ingegneria.uniparthenope.it/ricerca/Caterino_et_al_2013/). Four control algorithms, driving SA MR dampers, have been investigated through shaking table tests under seven different natural earthquakes. For each algorithm, a specific calibration has been done.

All of the considered control logics are able to change in real time the dynamical properties of the dampers according to the actual values of response quantities measured in the close surroundings of the dampers. The first one (Energy) aims to maximize the amount of energy extracted by an SA damper and needs a flexible connection between the device and floors among which the latter is installed. The second one (Modulated Homogeneous Friction - MHF) feeds the damper with a current proportionally to the last local maximum or minimum value of the 1st interstorey drift. The third control algorithm is referred to as "Sky Hook" since it aims to make the MR device mimics the behaviour of a damper constrained to the fixed space. The last investigated control logic (Acceleration Reduction) aims to minimize the amount of absolute accelerations in the main structure, i.e., to minimize the energy transmission from the ground to the structure through the SA brace. Three of these algorithms are of bang-bang (i.e., ON-OFF) type and do not need any parameter or structural model to work. Their calibration consist only in setting the minimum (i_{min}) and maximum (i_{max}) values of current to be given to the damper in the OFF and ON condition respectively. The other algorithm (MHF) belongs to the proportional type, feeding the damper with a current in the range [i_{min}, i_{max}] according to the instantaneous value of a specific response parameter. This logic is calibrated by setting the value of a gain constant, other than the i_{min} and i_{max} values.

The test campaign and the corresponding results lead us to the following conclusions:

1. Although many control algorithms proposed in literature try to include the electric dynamics of the circuitry inside MR dampers, the matter can be satisfactorily addressed through an appropriate control hardware. In this way, the reaction times of the electric circuitry inside the

damper can be set well beyond 1 ms and the global reaction times of the SA damper can be bounded to 10 ms, leading to a negligible effect of the damper's internal dynamics.

2. In real applications, variations of the force provided by a MR damper are smooth also for control algorithms corresponding to sharp variations of the current inside the damper.
3. The theoretical effectiveness of a control algorithm may be dramatically endangered by the number and the quality of on-line operations, such as measurement and processing. In particular, control algorithms relying on on-line measurement of non homogeneous quantities happen to be more prone to errors in the processing and command phases.
4. The experimental response reduction in terms of interstorey drift achieved by SA control system, compared to the bare, uncontrolled frame, can be close to 50% but can also be negligible, or even negative, depending on the amount of misoperations of the control algorithm adopted which, in turn, are directly related to its complexity. The response reduction in terms of floor acceleration can be even larger, but can also be negative.
5. Differently from passive control systems, reactive SA devices located only at few DOFs of a structure can increase the structural response at uncontrolled DOFs. This behaviour is dominated by the frequency content of the control action, rather than by its continuous or discontinuous nature.

A SA control system can significantly modify the total input energy coming into a structure from a ground motion. Therefore, such an energy cannot be taken as a constant in evaluating the dissipation capabilities of a SA control system.

Acknowledgments

The work behind this paper has been financially supported by the consortium Reluis with a grant by the Protezione Civile (Italian Emergency Agency). The MR dampers considered in this paper were designed, manufactured and provided for free by Maurer Söhne (Munich, Germany). The support of both is gratefully acknowledged.

References

Antonacci, E., De Stefano, A., Gattulli, V., Lepidi, M. and Matta, E. (2012), "Comparative study of vibration-based parametric identification techniques for a three-dimensional frame structure", *Struct. Contr. Health Monit.*, **19**(5), 579-608.

Basili, M., De Angelis M. and Fraraccio, G. (2013), "Shaking table experimentation on adjacent structures controlled by passive and semi-active MR dampers", *J. Sound Vib.*, **332**(13), 3113-3133.

Barroso, L.R., Chase, J.G. and Hunt, S. (2003), "Resettable smart dampers for multi-level seismic hazard mitigation of steel moment frames", *J. Struct. Control*, **10**, 41-58.

Bolt, B. (1969), "Duration of strong motion", *Proceedings of the 4th World Conference on Earthquake Engineering*, Santiago, Chile.

Cao, D., Song, X. and Ahmadian, M. (2011), "Editors' perspectives: road vehicle suspension design, dynamics, and control", *Vehicle Syst. Dynam.*, **49**(1-2), 3-28.

Caterino, N., Spizzuoco, M. and Occhiuzzi, A. (2011), "Understanding and modelling the physical behaviour of magnetorheological dampers for seismic structural control", *Smart Mater. Struct.*, **20**, 065013. Doi: 10.1088/0964-1726/20/6/065013

Caterino, N., Spizzuoco, M. and Occhiuzzi, A. (2013), "Promptness and dissipative capacity of MR dampers:

experimental investigations", *Struct. Control Health Monit.*, **20**(12), 1424–1440. Doi: 10.1002/stc.1578
Cha, Y.J., Zhang, J., Agrawal, A.K., Dong, B., Friedman, A., Dyke, S. J. and Ricles, J. (2013), "Comparative studies of semiactive control strategies for MR dampers: pure simulation and real-time hybrid tests", *J. Struct. Eng. - ASCE*, **139**(7), 1237-1248.
Crosby, M.J. and Karnopp, D.C. (1973), "The active damper", *Shock Vib. Bull.*, **43**, Naval Research Laboratory, Washington DC.
De Stefano, A., Matta, E. and Quattrone, A. (2008), *Dynamic identification of the JETPACS prototype*, Report 4/2008 Executive Project DPC-ReLUIS 2005–2008.
Dolce, M., Ponzo, F.C., Di Cesare, A., Ditommaso, R., Moroni, C., Nigro, D., Serino, G., Sorace, S., Gattulli, V., Occhiuzzi, A., Vulcano, A. and Foti, D. (2008), "Jet-pacs Project: Joint Experimental Testing on Passive and Semiactive Control Systems", *Proceedings of the 14th World Conference on Earthquake Engineering*, Beijing, China.
Erramouspe, J., Kiousis, P., Christenson, R. and Vincent, T. (2007), "A resetting stiffness dynamic controller and its bench-scale implementation", *Eng. Struct.*, **29**, 2602-2610.
Eurocode 8, UNI EN 1998-1 (2005), *Design of structures for earthquake resistance - Part 1: General rules, seismic actions and rules for buildings*.
Gattulli, G., Lepidi, M. and Potenza, F. (2009), "Seismic protection of frame structures via semi-active control: modeling and implementation issues", *Earthq. Eng. Eng. Vib.*, **8**(4), 627-645. Doi: 10.1007/s11803-009-9113-5
Inaudi, J.A. (1997), "Modulated homogeneous friction: a semi-active damping strategy", *Earthq. Eng. Struct. D.*, **26**(3), 361-376.
Inaudi, J.A. (2000), "Performance of variable-damping systems: theoretical analysis and simulation", *Structural Control for Civil and Infrastructure Engineering*, (Eds., F. Casciati and G. Magonette), World Scientific.
Jung, H.J., Jang, J.E., Choi, K.M. and Lee, H.J. (2008), "MR fluid damper-based smart damping systems for long steel stay cable under wind load", *Smart Struct. Syst.*, **4**(5), 697-710.
Jung, H. J., Spencer, B.F., Ni, Y.Q. and Lee, I.W. (2004), "State-of-the-art of semiactive control systems using MR fluid dampers in civil engineering applications", *Struct. Eng. Mech.*, **17**(3-4), 493-526.
Karnopp, D.C., Crosby, M.J. and Harwood, R.A. (1974), "Vibration control using semi-active Force Generators", *ASME J. Eng. Ind.*, **96**(2), 619-626.
Kobori, T., Takahashi, M., Nasu, T. and Niwa, N. (1993), "Seismic response controlled structure with active variable stiffness system", *Earth. Eng. Struct. D.*, **22**, 925-941.
Laflamme, S., Taylor, D., Maane, M.A. and Connor, J.J. (2011), "Modified friction device for control of large-scale systems", *Struct. Control. Health Monit.*, Doi 10.1002/stc.454
Lee, H.J., Jung, H.J., Moon, S.J., Lee, S.K., Park, E.C. and Min, K.W. (2010), "Experimental investigation of MR damper-based semiactive control algorithms for full-scale five-story steel frame building", *J. Intel. Mat. Syst. Str.*, **21**(10), 1025-1037.
Li, Z.-X., and Xu, L.-H. (2004), "Shaking-table test on semi-active control for seismic response of tall buildings using MRF-04K damper", *Proceedingsof the 13th World Conference on Earthquake Engineering*, Vancouver, B.C., Canada.
Occhiuzzi A. and Serino G. (2003), "A semi-active oleodynamic damper for earthquake control - Part 2: Evaluation of performance through shaking table tests", *Bull. Earthq. Eng.*, **1**(2), 275-302.
Occhiuzzi, A., Spizzuoco, M. and Serino, G. (2003), "Experimental analysis of magnetorheological dampers for structural control", *Smart Mater. Struct.*, **12**, 703-711.
Occhiuzzi, A. and Spizzuoco, M. (2005), "Experimental analysis of a semi-actively controlled steel building", *Struct. Eng. Mech.*, **19**(6), 721-47.
Ohtori, Y., Christenson, R.E., Spencer, B.F. and Dyke, S.Y. (2004), "Benchmark Control Problems for Seismically Excited Nonlinear Buildings", *J. Eng. Mech. - ASCE*, **130**(4), 363-582.
OPCM 3274, President of the Council of Ministers (2003), *Ordinance No. 3274 - First Elements Regarding the General Criteria for the Seismic Classification of the National Territory and Technical Standards for the Constructions in Seismic Zone* (in Italian).

Ponzo, F.C., Di Cesare, A., Moroni, C., Nigro, D., Ditommaso, R., Auletta, G. and Dolce, M. (2009), "JET-PACS: Joint Experimental Testing on Passive and semiActive Control Systems", *Proceedings of the L'Ingegneria Sismica in Italia – XIII Convegno Nazionale dell'ANIDIS*, Bologna, Italy.

Preumont, A. (2002), *Vibration control of active structures,* 2nd Ed., Kluwer Academic Publishers.

Sackman, J.L. and Kelly, J.M. (1979), "Seismic analysis of internal equipment and components in structures", *Eng. Struct.*, **1**(4), 179-190.

Sodeyama, H., Suzuki, K. and Sunakoda, K. (2004), "Development of Large Capacity Semi-Active Seismic Damper Using Magneto-Rheological Fluid", *J. Press. Vess. T. - ASME*, **126**, 105-109.

Stammers, C. W. and Sireteanu, T. (1998), "Vibration control of machines by use of semi-active dry friction damping", *J. Sound Vib*., **209**(4), 671-684.

Stammers, C.W. and Sireteanu, T. (2000), "Control off building seismic response by means of three semi-active friction dampers", *J. Sound Vib.*, **237**(5), 745-759.

Weber, F., Distl, H., Feltrin, G. and Motavalli, M. (2009), "Cycle energy control of magnetorheological dampers on cables", *Smart. Mat. Struct.*, **18**, 015005.

Xu, Y.L. and Chen, B. (2008), "Integrated vibration control and health monitoring of building structures using semi-active friction dampers: Part 1: methodology", *Eng. Struct.*, **30**(7), 1789-1801.

Yang, J.N. and Agrawal, A.K. (2002), "Semi-active hybrid control systems for nonlinear buildings against near-field earthquakes", *Eng. Struct.*, **24(2)**, 271-280.

Yang, J. N., Kim, J. and Agrawal, A. (2000), "Resetting semiactive stiffness damper for seismic response control", *J. Struct. Eng. - ASCE*, **126**(12), 1427-1433.

FC